

# Prediction of energy consumption of geologically different marble deposits in ground calcium carbonate (GCC) production

KAMAR SHAH ARIFFIN

School of Materials and Mineral Resources Engineering  
University Science Malaysia, Engineering Campus  
14300 Nibong Tebal, Pulau Pinang

**Abstract:** Ultrafine grinding to produce ground calcium carbonate (GCC) is an energy intensive process, even though only a small portion of the energy expended is directly applied to the size reduction of the particles. This study shows that the breakage rate is higher for coarser feedstocks, and that wet grinding reduces the tendency towards particle agglomeration. Material from Gunung Rimau (GR) requires more energy to grind than does material from Gunung Lano (GL). The difference can be attributed to the presence of minute size of flaky phlogopite crystals in the GR material. The Bond's Work Index (BWI) for GL and GR materials were measured at 32.16 and 31.6 kW/t respectively. General energy requirements for both fall within the range of 16 and 52 kWh/t, depending on the desired particle size distribution of the final product. The ultrafine grinding of GR material can consume as much as twice as much energy as does the ultrafine grinding of GL material, given identical final particle characteristics. Modeling of the process gives a good correlation between experimental values, and values calculated using the Charles' Size-Energy Reduction Theory. Differences in energy requirements, resulting from differences in the mineralogical composition of marbles, can therefore be significant, and should be taken into account when evaluating materials for exploitation.

**Abstrak:** Pengisaran dalam penghasilan serbuk kalsium karbonat (GCC) adalah proses yang memerlukan tenaga intensif dan hanya sejumlah kecil sahaja secara mekanik, akhirnya dimanfaatkan dalam proses pengurangan saiz. Kajian menunjukkan kadar penghancuran adalah tinggi bagi suapan bersaiz kasar. Kecenderongan zarah-zarah untuk tergumpal adalah sangat tinggi bagi pengisaran kering berbanding keadaan basah. Gunung Rimau (GR) dengan ciri-ciri fizikal berbeza sering memerlukan input tenaga pengisaran yang lebih tinggi berbanding Gunung Lano (GL). Ini dipercayai berpunca daripada kehadiran empingan-empingan kecil mika (palogofit) yang kaya dengan Mg, dan juga silika. Nilai Indek Kerja Bond bagi GL dan GR, masing-masing ialah 32.16 dan 31.6 kWh/t. Purata tenaga pengisaran bagi keduanya ialah dalam julat 16 hingga 52 kWh/t, bergantung kepada saiz taburan zarah akhir. Tenaga pengisaran yang diperlukan oleh bahan GR adalah 1 hingga 2 kali ganda lebih tinggi berbanding GL dalam menghasilkan produk yang berciri serupa. Percubaan permodelan telah mendapati perhubungan yang baik antara nilai ujikaji dan kiraan empirikal berdasarkan teori pengurangan saiz-tenaga Charles. Adalah disimpulkan bahawa kedua-dua enapan marmar berlainan ini mempunyai keperluan tenaga pengisaran yang berbeza dan perlu diambil kira dalam proses penilaian.

## INTRODUCTION

The production of fine and ultra-fine materials is an increasingly important and, at times, a critical process in the production of industrial minerals. Improved grades of ground calcium carbonate (GCC) are prized as fillers, and are found in many finished products. Mean particle size is one of the most critical of the physical properties of a carbonate filler, and for this reason, care must be taken during the grinding process.

Calcium carbonate materials are subjected to processes that involve crushing, pulverising and grinding to achieve several objectives:

- The production of fine to ultrafine ground calcium carbonate.
- The production of materials with narrowly defined particle size ranges and/or particle aspect ratios. Size ranges are expressed in terms of maximum, minimum and mean particle sizes.
- Materials with fine particle sizes are used where necessary to promote rapid chemical reactions, through

the exposure of large surface areas to reactants.

- To liberate valuable components from gangue or impurities for further beneficiation (e.g. by screening, high intensity magnetic separation, or flotation)

## OBJECTIVE

This investigation seeks to predict the particle size distribution of the ground product as a function of the operating conditions used during size reduction, and the energy expended in grinding process. In addition, it will examine the behaviour of materials when subjected to the selected processing system, and will focus on the detailed particle characteristics of the ground products.

## GRINDING MECHANISM THEORY

Comminution, is an operation involving the application of mechanical energy, and can be given three different definitions:

- (a) The reduction of large irregularly shaped solid particles

to smaller sizes.

- (b) The creations of new free surfaces.
- (c) The change in the number and size of particles, and the total particle surface area of the mass.

The choice of mill type, as well as several other factors, determine the effectiveness of the grinding operation, and the properties of the desired products (Orr, 1966; Hilton, 1983; Bosse, 1983; Chelik, 1988; Trass, 1990; Zheng *et al.*, 1995; Schneider, 1997). These may be summarized as:

1. Initial feed size and charge quantity of material.
2. Chemical and mineralogical composition of material.
3. The particle bonding associated with the material.
4. Material adhesive properties and moisture content.
5. Material hardness, strength and density.
6. Method of grinding — dry or wet (water or organic liquid).
7. Homogeneity and purity of material.
8. Solubility, toxicity, flammability, melting and abrasiveness of material.
9. Addition of grinding aids and media.

Abrasion tends to give a narrow size distribution, whereas impact produces a broad one and compression an intermediate one. In practice, these mechanisms do not occur in isolation, but one normally dominates. Compression is more likely to occur in crushers, impact in tumbling mills and abrasion in ultrafine grinding machines. Grinding is the fine phase of comminution or size reduction. Grindability is a measure of the rate of grinding of material to produce a certain amount of product size in a particular mill within a specified grinding time. Alternatively, grindability can be defined as the capability of a process to reduce an amount of material to a certain size per unit of input energy, or a measure of the resistance of the materials to the grinding process (Charles, 1957). Data from grindability tests are used to evaluate crushing and grinding efficiency.

The energy cost for an operating grinding plant, or the estimated expenditure for energy in a proposed crushing or grinding process, is a major determining factor in the success of the operation. Another aspect of the problem of energy comminution is the transfer of sufficient energy from the mover to the piece of material, causing it to fragment.

### Energy input in size reduction

The fine grinding process is characterized by non-first order breakage kinetics, so that the breakage rate decreases with longer grinding times. Various models have been introduced to surmount this problem (e.g. stochastic analysis) but all failed to anticipate the breakage rate required in the model (Duggirala and Fan, 1989). Given the lack of a satisfactory analytical model, an empirical correlation between energy and size reduction, Charles' Size-Reduction Relationship, is used instead. This energy-size reduction relationship has been demonstrated successfully, using differing approaches to the problem, and laboratory-scale mills (Agar, 1968; Herbst and Sepulveda, 1978; Ventakaraman, 1988; Gao and Forsberg,

1995). Typical figures for power consumption in fine grinding (between 125 mm - 1 mm) are 20-30 kWh/t and 100-1,000 kWh/t in superfine grinding.

Several methods have been suggested for calculating the relationship between size reduction and energy expended, based on differing theories of size reduction processes. Charles (1957) reported that the energy required to make a small change in the size of an object is proportional to the size change and is inversely proportional to the object size to some power of  $n$ . This concept is expressed as:

$$\partial E = -K(\partial d/d^n) \quad (1)$$

where  $\partial E$  is the input energy or energy change,  $K$  a constant,  $d$  the object's diameter, and  $n$  a constant.

According to this theory, for every comminution system, the specific energy input (kWh/t),  $E$ , expended in reducing a unit weight of uniformly sized material is related to the size modulus of the product,  $x_m$ , and can be mathematically generalized as:

$$E = Ax_m^{-a} \quad (2)$$

where  $a$  is the distribution modulus (slope of the log-log cumulative size distribution plot) and  $A$  is a constant primarily determined by properties of the material and grinding methods.

## EXPERIMENTAL METHODS

Batch grinding experiments were undertaken using a laboratory scale comminution device, in order to examine the particle size-power consumption relationship. The resulting particle size distributions were used to determine the kinetic parameters and energy requirements of the device at a pre-determined set of operating conditions and designed feeds.

### Raw materials

The study utilized two crystalline materials obtained from the state of Perak:

- (a) Gunung Lano (GL) — A pearly white to off-white based pink marble of Devonian age from Kinta Valley, Ipoh
- (b) Gunung (Gua) Rimau (GR) — A pale grey to greyish white silicified limestone of lower Devonian age from Upper Perak, near Lenggong.

**Gunung Lano (GL):** Fresh specimens of the rock show the typical characteristics of a high quality marble: brilliant pearl white in colour, hard, fine to medium grained texture, and massive. However, the rock actually found at Gunung Lano varies from white, to off-white and cream, due to contamination of the rock caused by the intense weathering and oxidation prevalent in hot, wet tropical climates. Traces of limonite and other iron oxides cause streaks and banding, especially along fissures and joints. The rock is composed of anhedral calcite crystals, which vary in size from fine to medium of several mm.

**Gunung Rimau (GR):** Fresh specimens of the rock are predominantly pale gray to grayish white in shade, with

streaks of grey to dark grey, massive, and fine to medium grained. Minute, lustrous, reddish to golden brown mica flakes are disseminated throughout, with concentrations common in some places. Pockets of coarse (less than 2 mm), creamy white minerals, occupying or filling irregular thin partings of the rock, are found locally. Limonite discoloration is common, especially along fissures and joints, where weathering action is intense. Presence of Mg-Al bearing tiny amount minerals such as phlogopite [ $\text{KMg}_3\text{AlO}_{10}(\text{OH}, \text{F})_2$ ], forsterite ( $\text{Mg}_2\text{SiO}_4$ ), spinel (which are products of dedolomitization), and cordierite ( $\text{Mg}_2\text{Al}_4\text{Si}_5\text{O}_{18}$ ) were in evidence. Traces of minerals with metallic luster, such as cubic pyrite, graphite and magnetite were also observed (Fig. 1).

## FINE GRINDING EXPERIMENTS

A McCrone micronising (vibrating) mill was employed in the production of filler-grade powder with a narrow particle size range, with minimum contamination, time and energy consumption. This laboratory scale mill is a compact vibratory, attrition mill powered by a 1/30 HP (24.5 watt) motor. The grinding canister consists of a 125 mm diameter cylindrical jar fitted with a screw-capped, gasketless, polythene closure as shown in Figure 2. The jar is packed with an ordered array of identical, cylindrical, grinding media of fine-grained, non-porous, polycrystalline corundum.

Test portions were subjected to wet grinding as well as a dry method. For wet grinding, the addition of isopropanol ( $\text{CH}_3\text{CHOHCH}_3$ ) as a grinding aid (supplied by Philip Harris Instruments, or Vicker's Laboratory) with density value of  $0.786 \text{ g/cm}^3$  and viscosity of  $2.41 \text{ mPa}\cdot\text{s}$  at  $20^\circ\text{C}$  were used. In this study, selected feedstocks from GL and GR were pulverised under the following test conditions:

- Similar feed size ranges while varying grinding times (10, 20, 30 and 40 minutes), and
- Different feed size ranges at constant times (10 or 20 minutes).

Figure 1 shows the physical appearance of typical Gunung Lano and Gunung Rimau materials in the form of slabs, cylindrical cores, crushed fragments and coarse-grained fractions. The chemical compositions of the materials are summarized in Table 1.

## RESULTS AND DISCUSSION

The following aspects, which normally govern the effectiveness of fine grinding operations, were investigated:

- Grinding time (T)
- Agglomeration effects
- Wet and dry grinding performance
- Morphology and aspect ratio
- Initial feed size (F)
- Quantity of feeds
- Energy consumption (E)

**Table 1.** Chemical composition of Gunung Lano and Gunung Rimau Marbles as compared to Bee Low limestone from UK.

Methods > Material	Wet analysis (%)		Bee Low* limestone
	GL	GR	
$\text{SiO}_2$	0.03	0.678	0.64
$\text{Fe}_2\text{O}_3$	0.0352	0.082	0.05
$\text{Al}_2\text{O}_3$	0.094	0.424	0.11
CaO	54.71	53.41	55.09
MgO	0.97	0.48	0.37
MnO	0.017	0.015	0.02
CuO	Traces	Traces	4ppm
Pb	12.6ppm	7.2ppm	10ppm
$\text{CaCO}_3$	97.64	96.4	-na-
$\text{MgCO}_3$	1.68	1.18	-na-
Total Carbonate	98.92	96.52	-na-
Grade (BGS Scheme, 1992)	High Purity	Medium	-na-
$\text{SiO}_2 + \text{Al}_2\text{O}_3 + \text{Fe}_2\text{O}_3$	0.1952	1.184	-na-
Matter Soluble in Acetic Acid	1.86	1.01	-na-
Moisture content	very low	very low	-na-
Carbonaceous matter	traces	traces	-na-
Acid Insoluble (HCl)	0.09 - 0.14	0.80- 1.21	-na-
Loss on Ignition at $1000^\circ\text{C}$	42.63	42.42	-na-

## Particle size distribution

Figures 3 and 4 show the cumulative particle size distribution curves (PSD) of the comminuted products from Gunung Lano (GL) and Gunung Rimau (GR) at several pre-determined sets of grinding condition. A standard "Polcarb-90" material is also included for comparison. The cumulative undersize distributions always maintain the 'S-type' profile. An increase in the grinding time results in the S-shaped curve moving towards the finer end of the scale.

Table 2 shows the particle sizes at the various passing percentage diameters ( $D_{90}$ ,  $D_{80}$ ,  $D_{50}$ ,  $D_{20}$  and  $D_{10}$ ) of the PSD curves of the GL and GR products, together with their respective Sharpness Indices. The Sharpness Index is based on the slope of a PSD curve, and is a measure of the degree to which the size distribution of particles within the sample differs from the mean particle size. The Sharpness Index is calculated using the ratio between the two percentile point diameters of PSD at some distance to each other such as  $D_{80}/D_{20}$ . A sharpness index of one would show a PSD being a vertical line and it is considered as a useful indicator of grinding efficiency of a mill for a given set of grinding condition.

## Grinding time

The amount of fines generated with the McCrone Micronising Mill is increases proportionally with time of grinding, irrespective of the initial feed size range. The derivation of new particles with the disappearance of larger particle sizes in the initial desired feed size ranges occurs continuously. As an example, in the case of GL product (GL-F2-20), the characteristic size,  $D_{80}$ , was reduced to  $20.5 \mu\text{m}$  after 20 minutes of grinding, as compared to 44

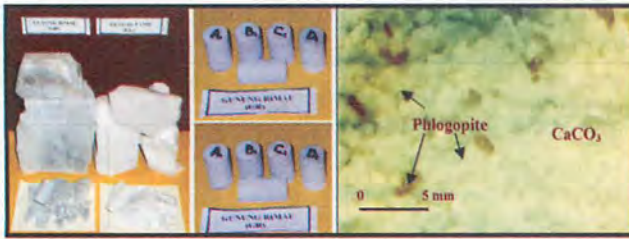


Figure 1. Typical crushed and coarse-grained fractions of the Gunung Lano and Gunung Rimau materials. Cut and polished slabs, and cylindrical core specimens of the marble from Gunung Lano and Gunung Rimau.

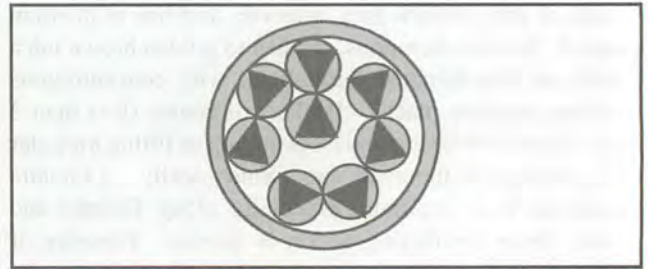


Figure 2. Cross section of grinding canister, showing movement of grinding elements (after McCrone Scientific Ltd., 1977).

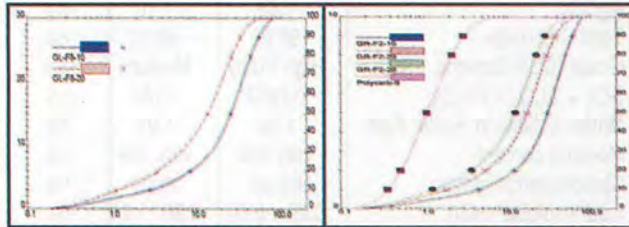


Figure 3. Cumulative undersize distribution curves of selective GL and GR feed sizes after subjected to 10, 20 and 30 minutes grinding time.

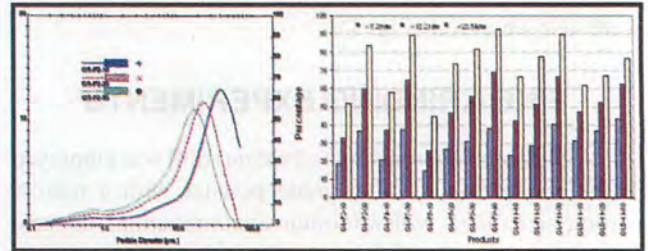


Figure 4. The frequency of the fine product distribution of GR marble obtained with the mill and (right) histogram of the Gunung Lano ground products reported at the three different particle sizes of 5.29 µm, 12.2 µm and 22.84 µm (GLD-dry grinding products).

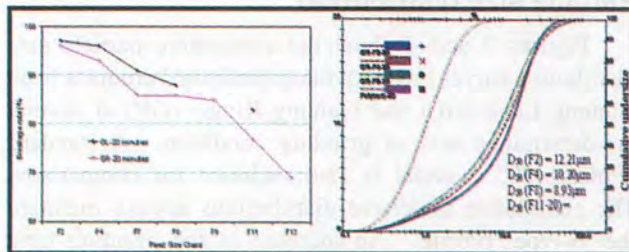


Figure 5. (Left) Size reduction rate of the GL and GR materials at different initial feed sizes after grinding for 20 minutes. (Right) Grain size distribution of the GR fines obtained using different feedstock size range for 30 minutes.

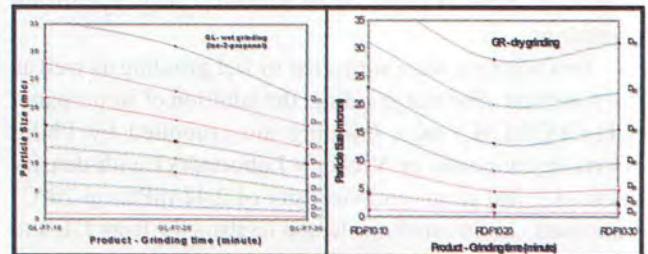


Figure 6. Effect of agglomeration on breakage rate and generation of ultrafine material with grinding time.

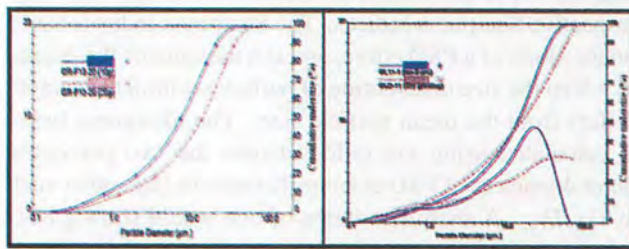


Figure 7. (Left) Particle size distribution of products ground at two different feed loads of 10 and 20 g. (Right) Size distribution curves a) 'S-type' - wet grinding and b) 'C-type' - dry grinding obtained using the McCrone micronising mill.

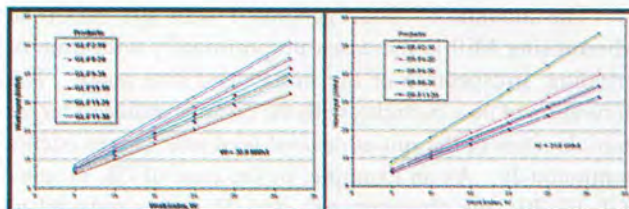


Figure 8. Linear relationship of presumptive work index with  $W_p$  obtained from the Tamrock brittleness test.

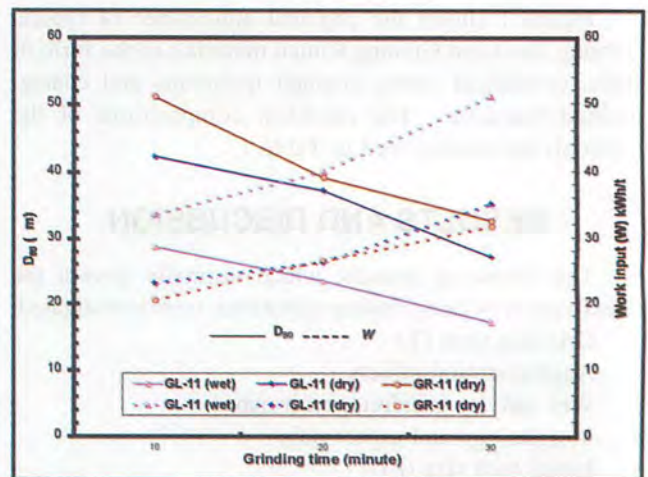


Figure 8a. Relationship of work input,  $W$  and characteristic size,  $D_{80}$  of dry and wet ground products of GL-11 and GR-11 for 10, 20 and 30 minutes.

**Table 2.** Characteristic size and sharpness index of the particle size distribution of the McCrone micronising mill products using iso-2-propanol. *Note:* GL-F2-10 means the product is G. Lano (GL), feed (F2) ground for 10min.  $x$  – average feed size, GLD: dry grinding products (GL).

Products	Feed size ( $\mu\text{m}$ )	$D_{90}$	$D_{80}$	$D_{50}$ ( $\mu\text{m}$ )	$D_{20}$	$D_{10}$	Sharpness ( $D_{80}/D_{20}$ )
GL-F2-10		55.0	44.0	20.5	5.9	2.0	7.4
GL-F2-20	F2	28.0	20.5	9.0	2.1	0.9	9.8
GR-F2-10	(600-710)	60.0	51.0	30.0	11.0	3.4	4.6
GR-F2-20	$x=655$	36.1	27.0	14.1	5.1	1.29	5.3
GR-F2-30		28.9	22.0	12.5	3.5	1.1	6.3
GL-F4-10	F4	49.6	38.7	19.4	5.0	1.7	7.7
GR-F4-20	(425-500)	43.0	32.0	16.6	4.7	1.6	6.8
GR-F4-30	$x=462$	30.6	21.1	10.4	2.8	1.0	7.5
GL-F7-10	F7	36.0	29.9	13.1	3.5	1.25	8.5
GL-F7-20	(250-300)	32.0	25.0	11.0	3.0	1.0	10.5
GL-F7-30	$x=275$	22.5	17.0	8.53	1.5	0.79	11.3
GR-F7-20		41.0	38.0	18.0	5.3	1.9	7.2
GL-F8-10	F8	55.6	45.0	25.61	8.2	2.84	5.4
GR-F8-20	(210-250)	33.2	26.0	13.5	3.2	1.11	8.1
GR-F8-20	$x=230$	42.5	32.0	17.4	5.0	1.92	6.4
GR-F8-30		27.6	20.0	8.93	2.2	0.9	9.1
GL-F9-30	F9	29.4	22.2	10.5	2.8	1.05	7.9
GL-F9-40	(180-210)	21.0	16.2	7.78	2.0	0.79	8.1
GR-F9-20	$x=195$	36.0	28.2	12.0	3.6	1.0	7.8
GL-F11-10	F11	36.3	28.4	14.1	3.8	1.3	7.4
GL-F11-20	(125-150)	31.9	23.2	11.8	3.1	1.3	7.5
GR-F11-20	$x=137$	40.8	31.2	16.0	4.2	1.4	7.4
GR-F13-20	F13	35.2	27.0	13.5	3.4	1.22	7.9
GR-F13-30	(75-106)	23.0	18.0	9.4	2.2	0.93	8.1
	$x=90$						
GR-F14-10	F14	41.1	33	16.0	5.2	1.60	6.3
GR-F14-20	(<75)	25.2	20	10.6	2.3	0.83	8.7
	$x=37$						

$\mu\text{m}$  after 10 minutes. After 20 minutes, no particles larger than 28  $\mu\text{m}$  were present, whereas after 10 minutes, 28  $\mu\text{m}$  represented  $D_{90}$ .

The breakage rates of GL material were relatively lower than those for GR. After 20 minutes of grinding, the F2 size fraction of GR (GR-F2-20) at  $D_{80}$  was 27.5  $\mu\text{m}$ , whereas with GL (GL-F2-20), the size was reduced to 20.5  $\mu\text{m}$ . The GR-F2 feed required a longer period of grinding (30 minutes) to attain the same  $D_{80}$  value as did GL-F2 after 20 minutes. Tiny flakes of golden brown mica (phlogopite) in the GR samples may have affected the grinding process of the material. Phlogopite rates 2.5-3.0 on Moh's Hardness Scale, and its density is 2.7-2.9  $\text{g}/\text{cm}^3$ , possibly affecting the homogeneity of the sample feed and interfering with the grinding of the  $\text{CaCO}_3$  component.

### Effect of feed size

Figure 5 presents the PSD curves of GR products obtained from feeding the mill with starting material of three different size ranges (F2, F4, F9) and grinding for 30 minutes. Characteristic sizes,  $D_x$  ( $x$ : 50%-90%) from these PSD curves, and sharpness indices of the distribution curves (as summarized in the Table 1) suggest that:

- The particle size of products at these percentile points, in general, decreased proportionally with the initial size range of the feed. However, the initial size range

of the feed material had only a slight effect on the mean product particle size range. For example, when compared with the GR-F2 feed, the mean particle sizes ( $D_{50}$ ) of GR-F4, GR-F8 and GR-F13 were reduced by 16, 28 and 24 percent, respectively.

- The influence of increased grinding time on the size reduction rate is relatively higher with the coarser grades of feedstock.  $D_{80}$  values for each initial feed size are shown in Figure 5. This may be attributable to the elimination of large flaws in small particles, and an increase in particle strength.

Since the rate of breakage decreases with particle size, a point of diminishing returns is reached, where further increases of grinding time do not result in significant increases in fineness. At this point, agglomeration is evident, hindering further breakage. Figure 6 shows that, for product sizes less than  $D_{50}$ , the rate of breakage gradually decreases and diminishes towards  $D_{10}$ , regardless of grinding time or feed size. The addition of isopropanol eases product handling, and enhances size reduction, perhaps by attacking weak microcracks in particles. It also serves as a dispersing surfactant, minimizing particle agglomeration.

The kinetic breakage rate is higher in products with a higher diameter range of  $D_{60}$ - $D_{90}$ . The rate of breakage eventually decreases, and again, a point of diminishing returns is reached. The plotted line becomes almost flat, and the size reduction rate approaches zero. Again, the addition of isopropanol enhances the breakage rate, as seen for the products of GL-F7 (Fig. 6). Dry grinding can actually lead to the phenomenon of size enlargement, caused by the agglomeration of fine particles.

### Feed quantity

The proportion of finer particles produced was higher when the quantity of feed charge was reduced by half. For example, the  $D_{50}$  of GR-F13 with 10 and 20 g loads after each was ground for 20 minutes was reduced to 12 and 8  $\mu\text{m}$ , respectively, as shown by Figure 7.

## ENERGY CONSUMPTION

Attempts to establish the energy consumption of the grinding operation using the McCrone micronising mill were made by means of the Bond third theory and Charles' energy-size reduction laws.

### Bond work index

The Bond work index method is the most widely used in the determination of grindability of materials and their energy requirements (Deister, 1987). However, Bond's method to determine grindability is time consuming, and a constant value is only achieved after several grinding periods. To date, there have been attempts to establish the Bond work index,  $W_i$ , using other grinding performance indicator methods, such as the Protodyakonov coefficient,  $f$  (Kaliampakos *et al.*, 1996), and the Tamrock brittleness friability number,  $S_{20}$  (Ozkahraman and Sirin, 1998).

**Table 3.** Selection of Bond work indices ( $W_i$ ).

Material	Specific gravity	Work index (kWh/t)	Reference
Limestone	-	12.74	Wills, 1988
	2.65	14.00	Lowrison, 1974
	2.65	12.5	Orr, 1966
Dolomite	-	11.27	Wills, 1988
	2.74	13	Lowrison, 1974
	2.74	11.3	Orr, 1966
Marble	2.71	4-12	Lowrison, 1974
	-	6-9.1	Kaliampakos <i>et al.</i> , 1996
	-	8-11	Ozkahraman & Sirin, 1998

Investigations by earlier workers have shown that the Bond work index for marble generally falls in a range of values from 4 to 12 kWh/t. Standard Bond work indices,  $W_i$  for typical limestone, marble and dolomite materials are presented in Table 3.

In this study, Bond work indices were determined using the Tamrock brittleness test as, described by Ozkahraman and Sirin, 1988, which is based on the empirical relationship between friability value ( $S_{20}$ ) obtained from the Tamrock test and Bond work index ( $W_i$ ) and grindability ( $G$ ) data. A linear relationship exists between  $G$  and  $S_{20}$ :

$$G = 0171 + 0.021(S_{20}) \quad (3)$$

and the relationship between  $W_i$  and  $S_{20}$  is:

$$W_i = 61.839 - 23.390 (\log S_{20}) \quad (4)$$

Average grindability values ( $G$ ) of GL and GR materials using the McCrone micronising mill were 0.57 and 0.59 g/rev in the case of a ball mill, and the corresponding Bond work indices ( $W_i$ ) were 32.0 and 31.6 kWh/t, suggesting that the  $W_i$  values for GL and GR are much higher than 14 kWh/t for marbles as shown in Table 3.

A comparative study was then conducted to demonstrate the relationship of the  $W_i$  values obtained from the Tamrock brittleness tests with a series of presumptive values of  $W_i$ . Work input ( $W$ ) values for various finely ground products from GL and GR were calculated using Bond's third theory of comminution formula. The  $D_{80}$  of the initial feed (F) particle size distribution was taken as 80% fineness within the linear range of the particular feeds (e.g.:  $D_{80}(F2) = 600 + (710 - 600) \times 0.8 = 680 \mu\text{m}$ ) and  $D_{80}$  values of the products (P) were derived from the respective size distribution curves.

Figure 8 shows work input ( $W$ ) of finely ground products of GL and GR at the various presumptive Bond work indices,  $W_i$  together with the  $W_i$  values obtained from the Tamrock brittleness test as calculated using the third Bond law. The relationship between energy requirement, product size and Bond work index are as follows:

- The work input expended to generate specific products, as denoted by the characteristic size  $D_{80}$  increases linearly with work index,  $W_i$ .
- The required work input increases proportionally with the fineness of the products, which is in turn dependent

**Table 4.** Energy consumption of the McCrone micronising mill.

Grinding time (minute)	Energy (kWh)	Specific energy feed : 20g (kWh/kg)
10	$4.083 \times 10^{-3}$	0.204
20	$8.167 \times 10^{-3}$	0.408
30	$12.250 \times 10^{-3}$	0.612
40	$16.333 \times 10^{-3}$	0.817
60	$24.500 \times 10^{-3}$	1.225

**Table 5.** Characteristic grain size at each passing percentile for GL-F8 and GL-F9.

Product >	GL-F8-10	GL-F8-20	GL-F9-30	GL-F9-40
Specific Energy, $E$ (kWh/t)	0.204	0.408	0.612	0.817
Characteristic size, $D_x$ ( $\mu\text{m}$ )				
$D_{90}$	55.6	33.2	29.4	21.0
$D_{80}$	45.0	26.0	22.2	16.2
$D_{50}$	25.6	13.5	10.5	7.78
$D_{20}$	8.2	3.2	2.8	2.0

**Table 6.** Regressed values of the parameters A and b for Figure 9.

Parameter	$D_{90}$	$D_{80}$	$D_{50}$	$D_{20}$	$D_{10}$
A	19.31	14.55	6.65	1.59	0.63
-b	0.6616	0.7041	0.8397	0.9829	0.889
R-squared	0.97	0.98	0.99	0.95	0.92

**Table 7.** Characteristic grain size at each passing percentile for GR-F2.

Products >	GR-F2-10	GR-F2-20	GR-F2-30
Specific Energy, $E$ (kWh/t)	0.204	0.408	0.613
Characteristic size, $D_x$ ( $\mu\text{m}$ )			
$D_{90}$	60	37	28
$D_{80}$	51	31	23
$D_{70}$	43	26	19
$D_{60}$	38	21	15
$D_{50}$	31	17	12
$D_{40}$	25	14	10.1
$D_{30}$	19	10	7.0
$D_{20}$	11	5.3	3.5
$D_{10}$	4.2	1.8	1.1

**Table 8.** Regressed values of the parameters A and b for Figure 10.

Parameter	$D_{90}$	$D_{80}$	$D_{70}$	$D_{60}$	$D_{50}$	$D_{40}$	$D_{30}$	$D_{20}$	$D_{10}$
A ( $\mu\text{m}$ )	19.916	13.286	15.874	9.885	7.856	6.720	4.462	2.094	0.605
-b	0.6932	0.7232	0.7406	0.846	0.863	0.8251	0.9095	1.0421	1.2182
R-squared	1	1	0.9997	0.9999	1	0.9999	0.9998	0.9999	1

on grinding time. As an example, GL-F11 products ground for 10, 20 and 30 minutes have resultant characteristic  $D_{80}$  values of 28.5, 23.2 and 17  $\mu\text{m}$ , respectively. The corresponding energy requirements to produce such products were 33.37, 39.86 and 51.04 kWh/t.

- Under similar conditions, GL materials require less work input than does GR material. For example, while work input for GR-F7-20 and GR-F11-20 were found to be relatively lower, the product sizes were somewhat coarser, than the equivalent GL products. To achieve the same grain sizes, GR requires more work input. The presence of mica particles in GR may reduce energy transfer to the particles, and therefore, the effectiveness of size reduction (Fig. 8a)
- The effect of initial feed size range on the energy and size reduction is less significant with the McCrone micronising mill.

## An energy-size reduction relationship

The specific energy required to comminute a feed material using the McCrone micronising mill can be represented by the following expression (Ventakaraman, 1988):

$$E = Pt/H \quad (5)$$

where P : power drawn by the mill (kW)  
t : required grinding time (hour)  
H : solid charged to the mill (kg or tonne)

This expression relates the energy expended per unit weight of the feed material ground with the mill to a desired fineness by the Charles energy-size reduction equation:

$$E = A (D_x)^{-b} \quad (6)$$

The Charles equation can also be expressed as:

$$\log E = -b \log D_x + \log A \quad (7)$$

This equation is an empirical expression relating a measure of the fineness of the comminuted products and the energy expended in operating the mill device, where

- E : specific energy (kWh/kg or kWh/t) expended in grinding a unit mass of the feed material to fineness products corresponding to the size modulus  $D_x$  or median size.  
 $D_x$  : the size modulus in the Gaudin-Schuman size distribution or median size or characteristic size (e.g.  $D_{90}$ ,  $D_{50}$  etc.).  
A : a constant, measuring how difficult it is to comminute the material (Breakage resistance).  
B : a constant, usually less than 1, also known as reduction rate.

This is one of the rational approaches available to determine and analyse the performance of comminution for fine grinding (Ventakaraman (1988), Goa and Forsberg (1995)). The Charles energy-size reduction relation is dependent only on the mill type, but independent of the mill size and its operating conditions. This method is suitable for short grinding time or low levels of grinding energy input and was used in this study. The specific energy,  $E$  (kWh/kg) was computed from the mill power (kW), the grinding time (h), and the solids,  $H$  (kg) hold-up in the mill. The McCrone micronising mill power ( $P$ ) is 1/30hp (24.5 watt). Results are shown in Table 4.

The Charles size-energy model above was used in this study in an attempt to predict product size distribution obtained from the McCrone micronising mill for GL and GR materials. This is the simplest method, since it only requires two parameters of characteristic size for size distribution prediction. The descriptive parameters  $A$  and  $b$  are determined from the experimental results. To determine the parameters  $A$  and  $b$  in the Charles equation, the particle size at each passing percentage,  $D_x$  (e.g.  $D_{90}$ ,  $D_{80}$  ...  $D_{10}$ ) from PSD curves are correlated to the specific energy ( $E$ ).

Table 5 and Figure 9 present the characteristic sizes at each passing percentage for the fine ground products GL-F8 and GL-F9. The products were ground for 10, 20, 30

and 40 minutes, respectively at a feed charge capacity of 20g. The resulting plot of energy versus size of the products on a log-log scale yields a series of straight or linear lines at each characteristic size,  $D_x$ . The regressed values of parameters  $A$  and  $b$  in the Figure 6 are tabulated in Table 8. Similar approaches were also applied to GR material with a coarser feed size range, F2, as shown in Table 7, Figure 10 and Table 8.

Figures 9 and 10 show that the PSD results for GL and GR correlate well to the Charles size-energy reduction equation over the whole range of characteristic sizes.

The overall size estimation using the Charles size-energy reduction was then calculated for each grinding time corresponding to the energy expended in the milling process by applying these parameters. Figure 11 shows the harmonization between experimental and calculated values of PSD for the mill obtained using Charles's law. Generally, these size-energy figures demonstrate that the energy expended increases proportionally with particle size reduction. Required work input increases proportionally with decreasing characteristic size,  $D_x$ . By applying this size-reduction equation, the parameters  $A$  and  $-b$  were determined for each characteristic size,  $D_x$  (Table 6 and 8). Figure 12 indicates that the overall feed size range has a small effects on size reduction. Effects of agglomeration may also reduce the reduction rate (<20%), as seen in the GL-F8/F9 materials, which have a finer feed fraction than GR.

## CONCLUSION

The percentage of size reduction, or breakage rate, is higher at coarser feed sizes. The overall effect of feed size upon the generation of very fine particles with similar grinding time is less obvious. The characteristic sharpness index of size distribution is generally higher with decreasing feed size range and grinding time, in both wet and dry grinding. The tendency for particles to agglomerate is pronounced with dry grinding, longer grinding times and fine feed sizes. This phenomenon causes serious difficulties in product handling when compared to wet methods using isopropanol. Dry grinding often exhibits a higher sharpness index,  $D_x$  than wet grinding, and normally shows little change when the grinding time was prolonged. Microscopic examination shows that the particles of these products are block like, irregular, angular to sub-angular in appearance, and resembled the initial feed with a tendency to break preferentially along rhombohedral cleavage planes. The particles in these products were frequently left with scratch marks on the fragmented surfaces. Generally, the overall grindability performance of GL materials was excellent, irrespective of any pre-set grinding conditions, and finer size reduction was achieved with less effort when compared to GR materials. The presence of mica flake (*phlogopite*) with different physical characteristics within the feed may have affected the fine grinding efficiency of the GR materials. Aspect ratios of both products were generally

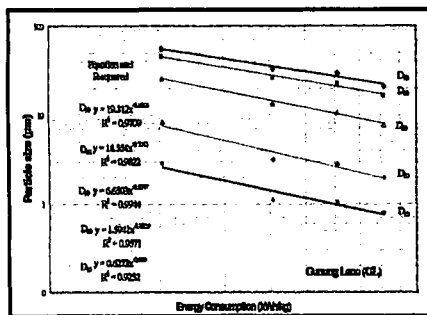


Figure 9. Characteristic particle sizes at different mass passing vs energy consumption for GL-F8.

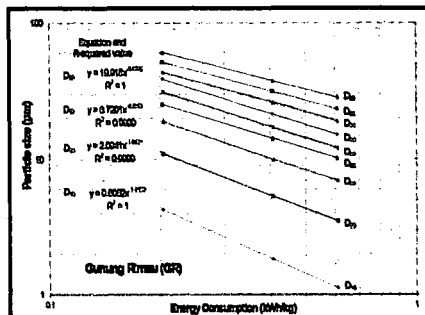


Figure 10. Characteristic particle sizes at different mass passing vs energy consumption for GR-F2.

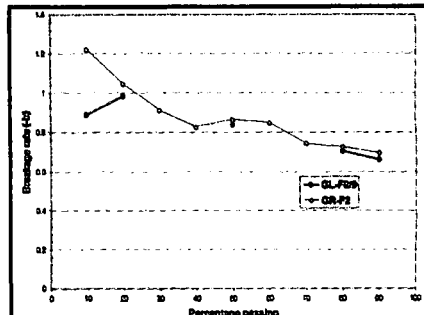


Figure 12. Variation rate of breakage with different feed size of GL and GR.

less than 2:1

Bond work indices of GL and GR materials were calculated at 32.0 and 31.6 kWh/t respectively. Work input or energy expended to generate specific products increased proportionally with corresponding initial feed size range, grinding time and wet versus dry grinding. Based on the Bond comminution law, the energy requirements for both products fell in the range 16.00 to 52.00 kWh/t. Energy requirement for GR products to attain a similar product size were apparently 1 to 2 times higher than those for GL materials.

Modeling was attempted to show product distribution by empirical relation to Charles size-energy reduction. The data indicated a good correlation between particle size distribution determined experimentally and calculated. Breakage rates for both materials also displayed similar trends, irrespective of their initial feed size; coarser feed sizes tended to have higher breakage rates, which were dramatically reduced when grinding proceeded.

## REFERENCES

- AGAR, G.E., 1968. Grindability and the determination of energy-size parameters. *Trans. Society of Mining Engineers AIME*, 241, 384-388.
- BOSSE, D.G., 1983. Ultrafine grinding, equipment types, capabilities, and choice. In: Malghan, S.G. (Ed.), *Ultrafine Grinding and Separation of Industrial Minerals*. AIME, New York, 3-8.
- CHARLES, R.J., 1957. Energy-size reduction relationships in comminution. *Trans. AIME*, 80-88.
- CHELIK, M.S., 1988. Acceleration of breakage rates of anthracite during grinding in a ball mill. *Powder Technology*, 54. Elsevier, Netherlands, 227-233.
- DEISTER, R.J., 1987. How to determine Bond work index using lab ball mill grindability tests. *Engineering and Mining Journal*, February, 1987, 42-45.
- DUGGIRALA, S.K. AND FAN, L.T., 1989. *Powder Technology*, 57. Elsevier Science, Netherlands, 1-20.
- GAO, M. AND FORSSBERG, 1995. Prediction of product size distributions for a stirred ball mill. *Powder Technology*, 84, 101-106.
- HERBST, J.A. AND SEPULVEDA, J.L., 1978. Technical Program, in Int. Powder and Bulk Solids Handling and processing.
- HILTON, W., 1983. Energy conservation in comminution systems. *IM Energy Supplement, Industrial Mineral*, London.
- KALIAMPAKOS, D.C., MOUTSATSOU A.K. AND SKOTARAS, J.K., 1996. Evaluation of wastes from marble quarries as paint fillers. *Trans. Inst. Min. Metall (Sect. C Mineral Process. Extr. Metal)*, 105, C37-C42.
- LOWRISON, G.C., 1974. *Crushing and Grinding, The size reduction of solid material*, London, Butterworths, 248.
- MCCRONE SCIENTIFIC LIMITED, 1997. The McCrone micronising mill and sample preparation kit manual. London, McCrone Research Associates, 8.
- ORR, C., JR., 1966. *Particulate Technology*. The Macmillan Co., New York, 562p.
- OZKAHRAMAN, T. AND SIRIN, M., 1998. The use of brittleness test in determination of grindability and crushing, In: Atak, Onal and Celik (Eds.), *Innovations in Mineral and Coal Processing*. Balkema, Rotterdam, 33-36.
- SCHNEIDER, B., 1997. Processing of ultrafine minerals. *Industrial Minerals*, October, London, 91-99.
- TRASS, O., 1990. Fine grinding of mica in the szego mill, *Powder Technology*, 60. Elsevier, Netherlands, 273-279.
- VENTAKARAMAN, K.S., 1988. Predicting the size distributions of fine powders during comminution, *Advanced Ceramic Materials*, 3(5), 498-502.
- WILLS, B.A., 1988. *Mineral Processing Technology, An introduction to the Practical aspects of ore treatments and mineral recovery*, 4th edition. Pergamon Press, U.K., 785p.
- ZHENG, J., HARRIS, C.C. AND SOMASUNDARAN, P., 1995. A study on grinding and energy input in stirred media mills, *Powder Technology*, 86. Elsevier, Science, Netherlands, 171-178.

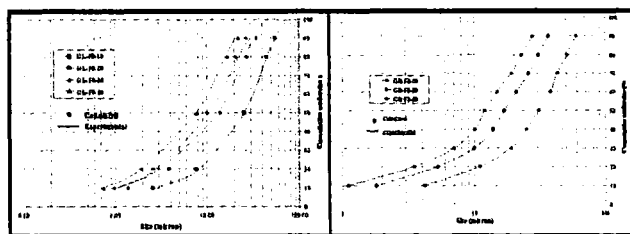


Figure 11. Calculated and experimental results of energy consumption of GL and GR products.